Geophysical Research Letters

RESEARCH LETTER
10.1029/2019GL082443

Seasonality of Intraseasonal Variability in Global Climate Models

M. Nakano[1] and K. Kikuchi[2]

[1]Japan Agency for Marine-Earth Science and Technology, Yokohama, Japan, [2]International Pacific Research Center, University of Hawai'i at Mānoa, Honolulu, Hawaii, USA

Key Points:
- The seasonality of two major modes of ISO (MJO/BSISO) in global climate models was examined
- Global climate models have larger deficits in their performances when representing the BSISO than the MJO
- The presented method helps in examining the model performance in detail and suggesting further improvements

Supporting Information:
- Supporting Information S1

Correspondence to:
M. Nakano,
masuo@jamstec.go.jp

Citation:
Nakano, M., & Kikuchi, K. (2019). Seasonality of intraseasonal variability in global climate models. *Geophysical Research Letters*, *46*, 4441–4449. https://doi.org/10.1029/2019GL082443

Received 14 FEB 2019
Accepted 9 APR 2019
Accepted article online 15 APR 2019
Published online 29 APR 2019

Abstract The tropical intraseasonal (30–90 days) oscillation (ISO) displays distinctive behaviors in boreal summer and winter. How well each mode is simulated in climate models has been investigated; however, very few studies have examined whether these modes are simulated in appropriate season. Here we developed diagnostics to assess this aspect and applied these diagnostics to numerous atmosphere-only and atmosphere–ocean-coupled models. We found out that all models share serious biases and that they sometimes incorrectly simulate the boreal summer ISO mode even in boreal winter and underestimate the appearance frequency of the boreal summer ISO in boreal summer. Nearly all atmosphere-ocean-coupled models show some improvements in the ISO seasonality representation compared to their atmosphere-only counterparts. It is suggested that good models for simulating the ISO seasonality have good life cycles for each ISO mode and that an accurate reproduction of the seasonal mean low-level zonal wind is crucial.

Plain Language Summary The leading intraseasonal (30–90 days) oscillation (ISO) in the tropical atmosphere has different characteristics in the boreal summer and winter. Accordingly, it has different impacts on extreme weather such as heavy precipitation and tropical cyclone activity. Many studies have examined how well the boreal summer and winter modes are simulated in climate models; however, very few studies have examined whether climate models can simulate the boreal summer and winter ISOs appropriately in the boreal summer and winter, respectively. In this study, we developed a new method to examine this aspect and applied it to numerous present-day climate simulations using both atmosphere-only and atmosphere–ocean-coupled models. We found out that all models share serious biases and that they inadequately simulate the boreal summer mode even in boreal winter and underestimate the appearance frequency of the boreal summer mode in boreal summer. Nearly all atmosphere–ocean-coupled models show some improvements in the ISO seasonality representation compared to their atmosphere-only counterparts. It is suggested that good models for simulating the seasonality of the ISO show good life cycles for each ISO mode and a seasonal mean zonal wind in the lower troposphere. These results are helpful for further improving climate models.

1. Introduction

The intraseasonal oscillation (ISO) is pronounced in the tropical atmosphere throughout the year. It is characterized by an eastward moving organized cloud envelope with a period of 30–90 days and a zonal extent of ~10,000 km. Observations show that the detailed evolution of ISO convection displays a significant seasonal cycle (e.g., Adames et al., 2016; Lau & Chan, 1985, 1986; Wang & Rui, 1990; Zhang & Dong, 2004). The ISO in boreal winter propagates along the equator and is often referred to as the Madden–Julian Oscillation (MJO) (Lau et al., 1988; Swinbank et al., 1988) in honor of its discoverers (Madden & Julian, 1971, 1972). Conversely, the ISO in boreal summer propagates not only eastward but also northward/northwestward over the northern Indian Ocean (IO) and the western North Pacific. This oscillation is sometimes called the boreal summer ISO (BSISO; Wang & Rui, 1990; Wang & Xie, 1997). Recent observational studies based on different approaches have confirmed this bimodal nature of the behavior of the ISO (Kikuchi et al., 2012; Kiladis et al., 2014; Szekely et al., 2016). The MJO mode occurs almost exclusively from December to April, whereas the BSISO mode occurs from June to October, with May and November being the transitional months.

It is of importance to represent this bimodal nature of the ISO in global climate models (GCMs), as well as to understand the underlying physics of how this mode selection operates, because not only is the ISO a

predominant phenomenon in the tropics but also it exerts a significant impact on a wide range of extreme weather events such as heat waves (Matsueda & Takaya, 2015), heavy precipitation (Jones et al., 2004; Ren et al., 2018; Xavier et al., 2014), tropical cyclone (TC) activity (Camargo et al., 2009; Klotzbach, 2014), and tornado outbreaks (Thompson & Roundy, 2013), with each ISO mode seeming to a play different role. For example, the BSISO has a more profound impact on TC activity in the northern IO and the western North Pacific (Kikuchi & Wang, 2010; Nakano et al., 2015; Nakazawa, 2006; Yoshida et al., 2014) and on the Asian summer monsoon onset and active/break cycles (e.g., Flatau et al., 2001; Pai et al., 2011; Wu & Wang, 2000) than does its MJO counterpart.

So far, different diagnostics have been proposed to assess various aspects of the ISO simulated in climate models (e.g., Ahn et al., 2017; Jiang et al., 2015; Kim et al., 2009, 2014; Neena et al., 2017; Wang et al., 2018). These diagnostics have been applied to various data sets and have succeeded in revealing common biases across models, such as weaker ISO amplitudes, very fast eastward propagation speeds, and poor representations of the northward propagation of the BSISO mode. The focus of these studies has been to better understand and reduce these biases, with a particular focus on the canonical behavior of each ISO mode. Few studies, however, have addressed how well the bimodal nature of the ISO is simulated by GCMs.

The purpose of this study is to assess in great detail the seasonality of the ISO simulated by a range of GCMs. We propose novel diagnostics to evaluate the model performance on the basis of the bimodal ISO representation concept devised by Kikuchi et al. (2012) and apply these diagnostics to numerous atmosphere-only and atmosphere–ocean-coupled climate simulations. Kikuchi et al. (2017) applied similar diagnostics to the Atmospheric Model Intercomparison Project (AMIP)-type simulation using a nonhydrostatic global model and found a major bias in the representation of the ISO seasonality. Our diagnostics aim to elucidate important aspects that have been ignored and are perhaps complementary to other diagnostics. The use of the Coupled Model Intercomparison Project phase 5 (CMIP5; Taylor et al., 2012) data set allows us to directly compare our results to those of previous studies (e.g., Ahn et al., 2017; Sabeerali et al., 2013), leading to a more comprehensive understanding of the simulated ISO in GCMs. We show that every GCM examined here has a serious problem in its representation of the ISO seasonality, which should be added to the list of major common biases in current GCMs that need to be greatly improved.

2. Data

We analyzed the first ensemble member data of 24 Atmospheric Model Intercomparison Project (AMIP) experiments and 18 historical experiments (hereafter referred to simply as CMIP) of CMIP5. Note that the observed sea surface temperature is prescribed in the AMIP experiments, whereas sea surface temperature is simulated by each climate model in the CMIP experiments. Most models have both CMIP and AMIP outputs; therefore, we were able to examine the impact of ocean coupling on simulating the ISO seasonality. We added an AMIP-type experiment using the nonhydrostatic global icosahedral model (NICAM; Tomita & Satoh, 2004; Satoh et al., 2008, 2014) which was performed by Kodama et al. (2015) in AMIP models because this model has unique features compared to the CMIP5 models; it has a higher horizontal resolution (14 km) and does not employ any convective parameterizations. Previous studies have shown that NICAM has a promising performance for forecasting ISOs and the related TC genesis (Miyakawa et al., 2014; Nakano et al., 2015, 2017). It is therefore expected that this model will also perform well for climate simulations. All models used in this study are listed in Table S1.

The National Oceanic and Atmospheric Administration interpolated outgoing longwave radiation (OLR) data (Liebmann & Smith, 1996) were used to extract the observed daily ISO modes (see section 3). The Japanese 55-year reanalysis (Kobayashi et al., 2015) was used to examine the dynamic and thermodynamic fields. Our analysis is based on 30 years (1979–2008) of data, except in the case of the CMIP simulations (1979–2005).

3. Analysis Method

To measure the state of the ISO on any given day, we follow the diagnostics developed by Kikuchi et al. (2012) and Kikuchi et al. (2017). In this method, an extended empirical orthogonal function (EEOF; Weare & Nasstrom, 1982) analysis with three lags of five-day intervals is performed on 25–90-day filtered OLR data in boreal summer (June–August) and winter (December–February). Then, the BSISO and MJO

principal component (PC) time series are calculated by projecting the 25–90-day filtered OLR onto the first two EEOFs of boreal summer and winter, respectively. The ISO mode for a given day is determined by selecting the larger norm mode between the BSISO and MJO PCs. If both norms are smaller than 1 standard deviation of the corresponding PCs during their target season, no ISO is identified for that day.

The BSISO and MJO PC time series for the models were also obtained in a similar manner by projecting the 25–90-day filtered simulated OLR onto the observed EEOFs. As discussed by Kikuchi et al. (2017), since we are interested in how models are able to accurately simulate the observed spatiotemporal structures of the ISO rather than in isolating the model's preferred spatiotemporal structures of the ISO, we do not use EEOFs derived from model simulations. Because the ISO simulated in the models is usually much weaker in amplitude, the PCs in the models are adjusted by dividing by α,

$$\alpha = \frac{\overline{\left\|\mathrm{PC}_{\mathrm{MJO}}^{\mathrm{model}}\right\|} + \overline{\left\|\mathrm{PC}_{\mathrm{BSISO}}^{\mathrm{model}}\right\|}}{\overline{\left\|\mathrm{PC}_{\mathrm{MJO}}^{\mathrm{obs}}\right\|} + \overline{\left\|\mathrm{PC}_{\mathrm{BSISO}}^{\mathrm{obs}}\right\|}},$$

before determining the ISO mode for a given day. That is, α is a measure of the ISO amplitude simulated by a model. This adjustment works well to identify nearly the same number of total ISO days per year as in the observation (~200 days/year).

To assess various aspects of the model performance, we employed the Taylor skill score (Taylor, 2001) throughout this study. The Taylor skill score (TSS), S, provides a single objective score of how well the observed and simulated spatial patterns or time series match each other and is defined as

$$S = \frac{4(1+R)^4}{(\sigma + 1/\sigma)^2 (1+R_o)^2},$$

where σ is the ratio of the standard deviations (model/observation), R is the correlation coefficient between the observations and a model, and $R_o = 1$.

4. Simulated ISO Seasonality

Figure 1 summarizes the seasonality in the ISO within the bimodal representation concept. Each bar shows the appearance frequency of each ISO mode in each month, and the model results are summarized in terms of the multimodel ensemble mean (MME), with the error bars representing the maximum/minimum intermodal variability. As in Kikuchi et al. (2012), the observation shows that the BSISO (MJO) is dominant in June–October (December–April) and that May and November are the transitional months. The MME reproduces the seasonal cycle in the ISO reasonably well, even though significant common biases are evident. First, a fraction of the significant ISO events in the models are more similar to the BSISO mode than the MJO mode even in the period of December–April (on average 26% in the AMIP models and 21% in the CMIP models). Kikuchi et al. (2017) reported that this is one of the major biases seen in NICAM AMIP-type experiments. We found out that all of the climate models examined here have this winter BSISO bias. Second, the appearance frequency of the BSISO in June–October is underestimated in MME (on average by 32% in the AMIP models and by 34% in the CMIP models). However, MME better represents the appearance frequency of the MJO in boreal winter with a slight underestimation but has a slight MJO bias in June–October (on average 14% in both the AMIP and CMIP models). These results indicate that current climate models share a major problem when representing the BSISO compared to the MJO. Third, all models underestimate the ISO amplitude. The α in the MME is 0.55 (which means that the simulated ISO amplitude is approximately half of the observed amplitude), and all models have α values smaller than 1. Note that the winter BSISO bias is slightly reduced and that the ISO amplitude is slightly larger in the CMIP models (0.61) compared to the AMIP models, suggesting that including air–sea-coupling processes improves the simulation of the ISO seasonality, as well as the amplitude, to some extent.

How does each model represent the ISO seasonality? Shown in Figure 2 are Taylor diagrams (Taylor, 2001) that summarize the ISO seasonality in the AMIP and CMIP models. Here we defined the frequency as the appearance frequency of the BSISO minus that of the MJO in each month and calculated the correlation between the observations and each model and the standard deviation of the frequency over 12 months.

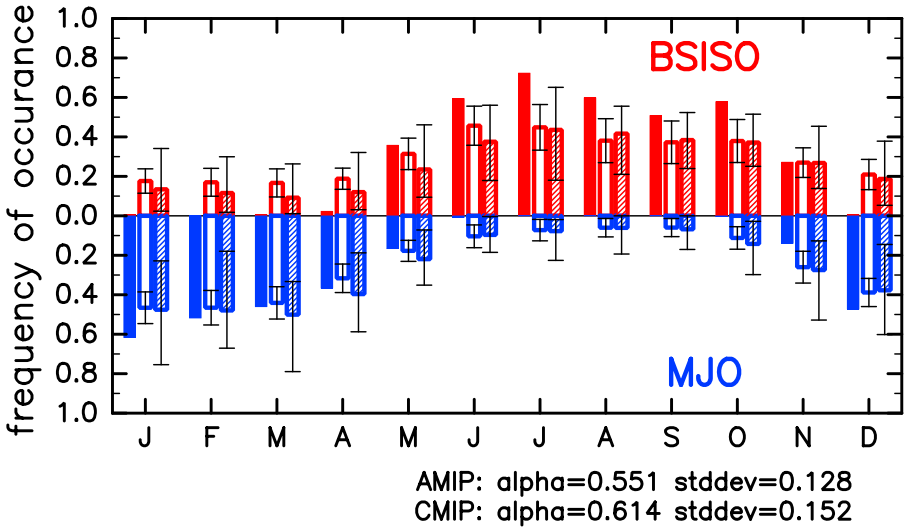

Figure 1. Monthly appearance frequency of the BSISO and the MJO. The solid, open, and striped bars represent the observation, AMIP, and CMIP, respectively. The error bars indicating the maximum and minimum intermodal variability.

The correlation coefficients, R, are relatively high for all models (over 0.7), and the ratio of the standard deviations (model/observation), σ, varies greatly with the model and is always smaller than the observations. These results indicate that every model simulates the phase of the ISO seasonality relatively well; however, their ability to simulate the MJO/BSISO contrast throughout the year is weaker and is highly variable between each model.

The CMIP MME has a higher TSS than the AMIP MME because of its larger standard deviation ratio. It is possible that the reduction in the winter BSISO bias (Figure 1) contributes to this. In nearly all models, the CMIP models have a higher TSS than the AMIP models (only two out of 17 models, namely, IPSL-CM5B-LR and MIROC-ESM, degrade the score). In particular, MIROC5 shows a remarkable improvement with a score increase of 0.57. CSIRO-Mk3.6, GFDL-CM3, and NorESM1-M also show moderate improvements (~0.3). Note that our assessment appears to be consistent with the conclusions of previous studies examining different aspects of the ISO. For example, Sabeerali et al. (2013) identified, somewhat

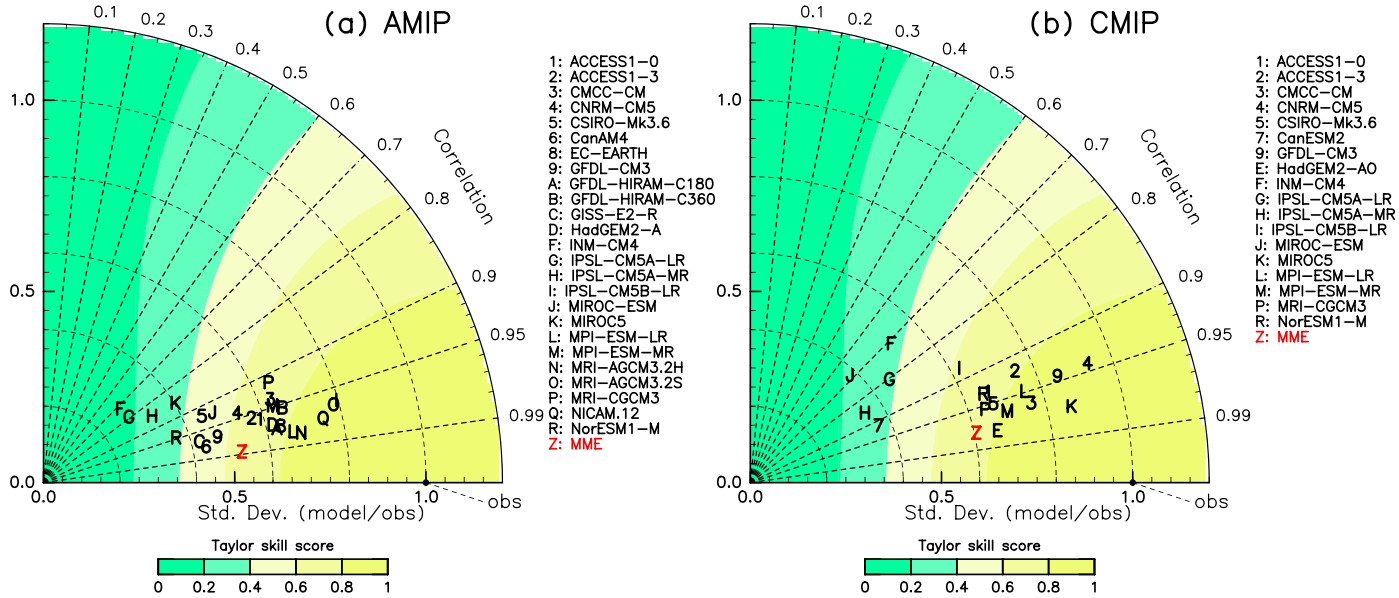

Figure 2. Taylor diagram for the monthly appearance frequency of the BSISO minus that of the MJO for the (a) AMIP and (b) CMIP models.

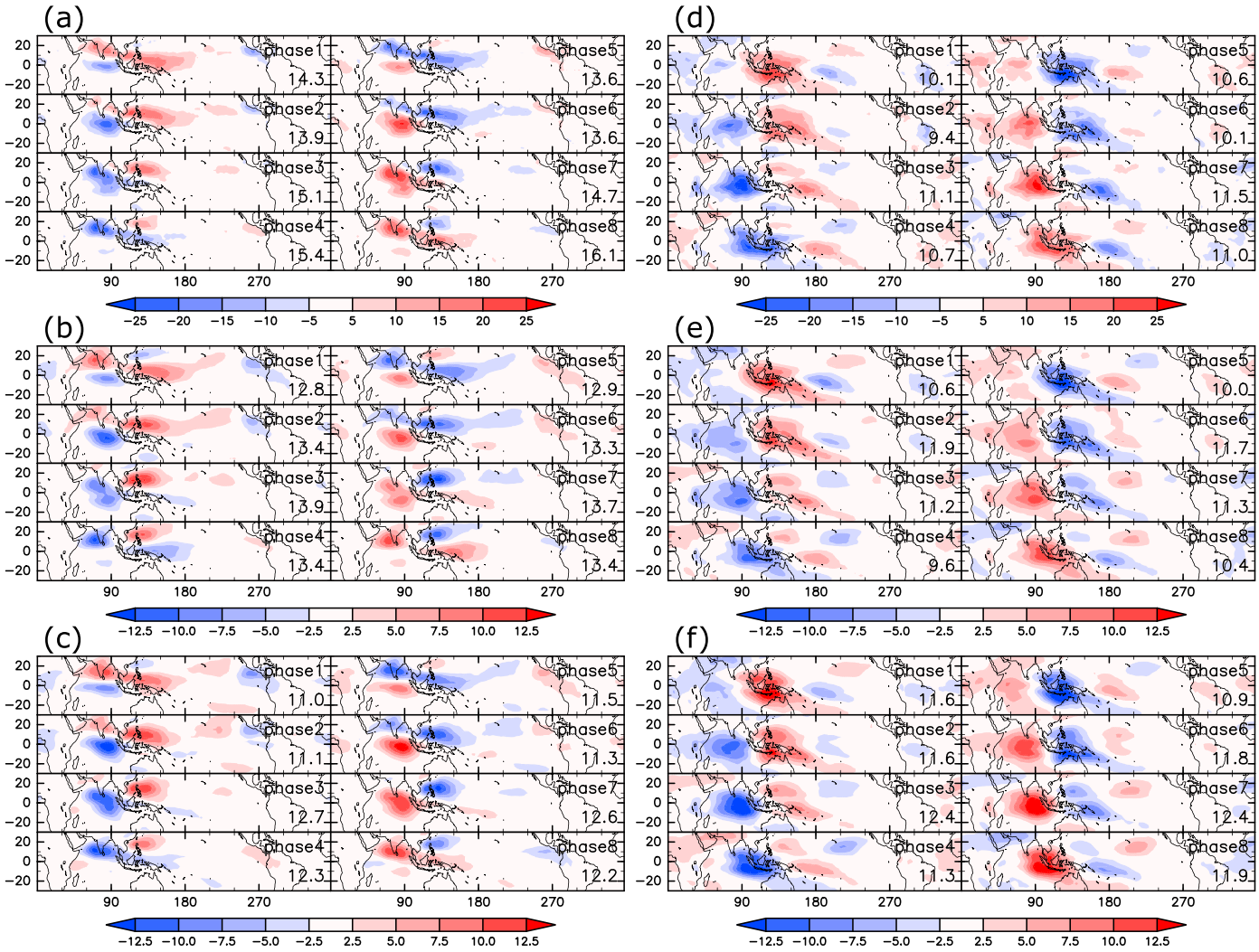

Figure 3. OLR anomaly (W/m^2) for the (a–c) BSISO and (d–f) MJO life cycles in the (a and d) observations, (b and e) AMIP MME mean, and (c and f) CMIP MME mean. Additionally, the average number of days per year for each phase is shown.

subjectively, five good models for simulating the BSISO (CMCC-CM, GFDL-CM3, IPSL-CM5A-LR, MIROC5, and MPI-ESM-LR). All of these models, except for IPSL-CM5A-LR, can be categorized as good models in terms of the seasonality (e.g., seasonality TSS > 0.8; see Table S1). Therefore, it is suggested that models that are able to simulate the ISO seasonality tend to be good at simulating other aspects of the ISO. In addition, it is suggested that including atmosphere–ocean-coupling processes improves the representation of the ISO seasonality.

Finally, we discuss why MIROC5 CMIP exhibits a significant improvement in the representation of the ISO seasonality, which should provide a better idea of how our diagnostic framework works to identify a model's deficiencies. The ISO seasonal cycles in both MIROC5 AMIP and CMIP (Figure S1) display similar bias tendencies as their corresponding MMEs (Figure 1), even though MIROC5 AMIP greatly exaggerates the tendencies and MIROC5 CMIP diminishes such tendencies. These models show very different abilities to simulate the intraseasonal variance of the OLR (Figure S2). Obviously, MIROC5 AMIP underestimates the variance of OLR in the IO and the tropical western North Pacific (e.g., 15°–20°N). These biases are significantly reduced in the CMIP model. These biases are, of course, related to the behavior of individual ISO events. As shown by Kikuchi et al. (2012), the BSISO amplitude is usually larger than the MJO amplitude in the boreal summer, and vice versa in the boreal winter (Figure S3), showing a clear bimodality. In the AMIP model, by contrast, the amplitudes of the MJO and BSISO modes in boreal summer tend to be comparable

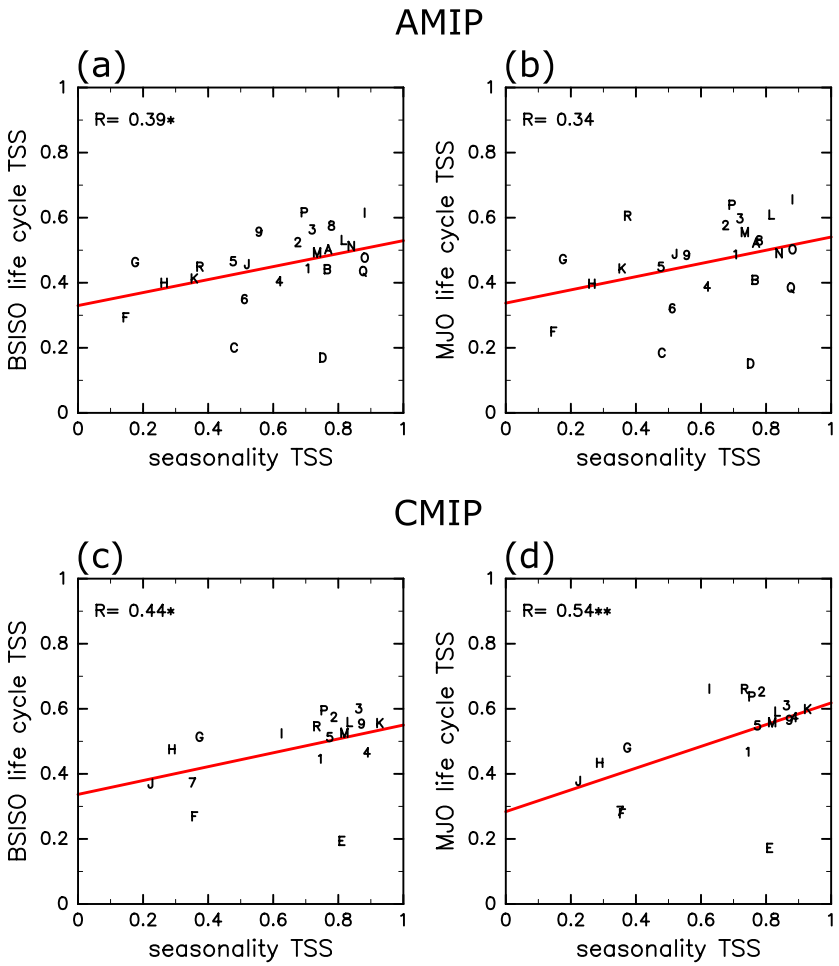

Figure 4. Scatter diagram of the Taylor skill score for the (a and c) BSISO and (b and d) MJO life cycle pattern composites versus the Taylor skill score of the ISO seasonality in (a and b) AMIP and (c and d) CMIP models. The correlation and linear regression lines are shown in each panel. The asterisks denote the statistical confidence level of the correlation (***>99%, **>95%, and *>90%).

(i.e., failing to reproduce the correct ISO behavior), whereas the model shows a relatively reasonable ISO behavior in boreal winter. It is evident that this boreal summer bias is significantly improved in the CMIP model. In addition, the representation of the ISO in boreal winter is improved (Figure S3).

5. Correlations With ISO Seasonality

This section discusses how a model's bias in the representation of the ISO seasonality is related to various aspects of the simulated ISO and backgrounds (e.g., the seasonal mean fields). It is obvious that the behavior of the ISO is closely tied to the background on which it is embedded. Therefore, it is reasonable to anticipate that a model's bias is related to the biases in the backgrounds. One may also be interested in the relationship between a model's ability to simulate the ISO seasonal cycle and to simulate the life cycle of each ISO mode. It is expected, from the results in the previous section, that these aspects are related. First, we address this question more in detail. As in many previous studies, we constructed OLR composites composed of eight phases (life cycles) of the BSISO and the MJO based on the PCs of each mode. Figure 3 shows the life cycles of the MME ISO. Although the MME reasonably reproduced the spatial pattern of each phase with a weaker amplitude (approximately one half), the life cycles simulated by each model show high diversity. For example, MIROC5 AMIP has difficulty simulating the ISO convection in the IO in both seasons, resulting in a failure to reproduce the slantwise structure of the BSISO and the convective organization of the MJO (Figure S4). This failure to reproduce the northwest-southeast elongated convective pattern is a common deficiency

in poor BSISO models (Sabeerali et al., 2013). By analogy with the above discussion, a TSS-based assessment was again conducted on the life cycles of the MJO and BSISO modes across all models. Figure 4 shows the relationship between the fidelity of the ISO seasonality and that of their life cycles in terms of TSS. These fidelities are positively correlated for both ISO modes, and the correlation coefficients are slightly higher than the 90% significance level for the AMIP experiments. For the CMIP experiments, the correlation coefficient is larger than the 90% (95%) significance level for the BSISO (MJO). Therefore, the models that reproduce better life cycles for the MJO and BSISO tend to produce a better seasonal cycle for the ISO and vice versa, particularly in CMIP models. In addition, note that models that reproduce the life cycle of the MJO better tend to also reproduce that of the BSISO better (not shown).

What aspects of the background mean state are related to the model performance for the ISO seasonality? Of the various aspects of the seasonal cycle, it is beyond doubt that the Asian monsoon system plays a central role. The Asian monsoon region is characterized by a strong easterly vertical wind shear and abundant moisture, which favor the development of the northward migration of the BSISO (e.g., Jiang et al., 2004; Wang & Xie, 1997). However, we cannot find any significant correlation between the vertical wind shear and ISO seasonality (not shown). Instead, it is the lower level zonal winds that appear to have a large impact. Figure S5a shows scatter diagrams of the TSS for the seasonal mean zonal wind pattern at 850 hPa (30°S–30°N) versus that for the ISO seasonality. Clearly, they are positively correlated. What about the relationship with moisture? Figure S5b shows scatter diagrams of the TSS for the seasonal mean specific humidity pattern at 850 hPa (30°S–30°N) versus that for the ISO seasonality. They are also positively correlated. These results indicate that an improved simulation of the lower tropospheric background circulation and humidity patterns, in general, leads to a better representation of the ISO seasonality (and possibly the life cycles). Why is an accurate representation of the mean moisture and zonal wind patterns important? There are likely several potential reasons. From the viewpoint of the importance of moisture advection (e.g.,Gonzalez & Jiang, 2017; Jiang et al., 2018; Sobel & Maloney, 2012, 2013), the mean moisture and zonal wind fields should be accurately represented, as well as their ISO components, to accurately simulate the moisture tendencies associated with the ISO. Another possible reason, particularly for the BSISO representation, is that an accurate representation of the mean zonal wind pattern is important because it determines the absolute vorticity distribution and its gradient, which may be responsible for the northward propagation of the vorticities (e.g., DeMaria, 1985), which are a major part of the northward propagating component of the BSISO.

A further, more in-depth, that is, process-oriented, analysis would help in identifying what controls the ISO seasonality and how to reduce the model biases associated with it.

6. Conclusions

A model's ability to simulate the ISO seasonality was examined for CMIP5 models and NICAM in the framework of the bimodal ISO concept (Kikuchi et al., 2012). That is, the ISO seasonality was summarized in terms of the monthly appearance frequency of the two major ISO modes (BSISO and MJO). We found out that all of the models examined here share serious biases in their representation of the ISO seasonality. The models incorrectly simulate the BSISO even in boreal winter (a winter BSISO bias) and underestimate the frequency of the BSISO in boreal summer. In addition, all models underestimate the amplitude of the ISO modes by nearly half on average. The models with high-performance levels for representing the ISO seasonality are likely to reproduce the life cycle of the ISO better throughout the year. It is suggested that an accurate representation of the background moisture and zonal wind in the lower troposphere is of particular importance.

Misrepresentation of the ISO mode on a given day of the year in climate models results in a number of potential weaknesses in model-based studies. For example, given that the ISO, particularly the BSISO, has a profound impact on the TC activity (e.g., Kikuchi & Wang, 2010; Nakano et al., 2015; Nakazawa, 2006; Yoshida et al., 2014), a misrepresentation of the ISO mode would lead to large uncertainties in the climate models, which would result in significant problems in future climate studies and subseasonal prediction studies, among others. Still, how such misrepresentations of the ISO mode in GCMs affect the representation of significant weather events (e.g., TC genesis or monsoon active/break cycles) is a completely open question and warrants further study. The positive result implied by our analysis is that efforts to better simulate the life cycles of the MJO and the BSISO lead to better representations of the ISO seasonality.

Acknowledgments

This study was supported by the Environment Research and Technology Development Fund (2RF-1701) of the Environmental Restoration and Conservation Agency of Japan (ERCA), the Integrated Research Program for Advancing Climate Models (TOUGOU), and the FLAGSHIP2020 project (proposal hp160230, hp170234, and hp180182) of the Ministry of Education, Culture, Sports, Science and Technology of Japan (MEXT) and JSPS KAKENHI grant 17K13010. The NICAM-AMIP simulation was conducted on the K computer (proposal hp120279, hp130010, and hp140219). This research was conducted under the JAMSTEC IPRC Joint Initiative (JIJI). The authors thank the NICAM development team for their fruitful discussions and data. K.K. acknowledges the support of NOAA CPO grant NA17OAR4310250. All figures were drawn using the GFD Dennou Club Library (http://www.gfd-dennou.org/library/dcl/), and Ryo Mizuta at the Meteorological Research Institute of Japan Meteorological Agency provided the library for drawing the Taylor diagram. The CMIP5 model data were provided by the Earth System Grid Federation (https://esgf-node.llnl.gov/projects/cmip5/). NOAA Interpolated OLR data provided by the NOAA/OAR/ESRL PSD, Boulder, CO, USA, from their Web site at https://www.esrl.noaa.gov/psd/. JRA-55 data produced by Japan Meteorological Agency are taken from https://jra.kishou.go.jp/JRA-55/index_en.html. NICAM-AMIP data and PC time series for all models used in this paper are available at https://doi.org/10.5281/zenodo.2563729. The Climate Data Operators (https://code.mpimet.mpg.de/projects/cdo/) were used for the data preprocesses. NICAM-AMIP type experiment data will be provided upon request. Contact the corresponding author for data availability. School of Ocean and Earth Science and Technology contribution 10680 and International Pacific Research Center contribution 1375.

References

Adames, Á. F., Wallace, J. M., & Monteiro, J. M. (2016). Seasonality of the structure and propagation characteristics of the MJO. *Journal of the Atmospheric Sciences*, *73*, 3511–3526. https://doi.org/10.1175/JAS-D-15-0232.1

Ahn, M. S., Kim, D., Sperber, K. R., Kang, I.-S., Maloney, E., Waliser, D., & Hendon, H. (2017). MJO simulation in CMIP5 climate models: MJO skill metrics and process-oriented diagnosis. *Climate Dynamics*, *49*, 4023–4045. https://doi.org/10.1007/s00382-017-3558-4

Camargo, S. J., Wheeler, M. C., & Sobel, A. H. (2009). Diagnosis of the MJO modulation of tropical cyclogenesis using an empirical index. *Journal of the Atmospheric Sciences*, *66*, 3061–3074. https://doi.org/10.1175/2009JAS3101.1

DeMaria, M. (1985). Tropical cyclone motion in a nondivergent barotropic model. *Monthly Weather Review*, *113*, 1199–1210. https://doi.org/10.1175/1520-0493(1985)113<1199:TCMIAN>2.0.CO;2

Flatau, M. K., Flatau, P. J., & Rudnick, D. (2001). The dynamics of double monsoon onsets. *Journal of Climate*, *14*(4), 130–146. https://doi.org/10.1175/1520-0442(2001)014<4130:TDODMO>2.0.CO;2

Gonzalez, A. O., & Jiang, X. (2017). Winter mean lower tropospheric moisture over the Maritime Continent as a climate model diagnostic metric for the propagation of the Madden-Julian Oscillation. *Geophysical Research Letters*, *44*, 2588–2596. https://doi.org/10.1002/2016GL072430

Jiang, X., Adames, Á. F., Zhao, M., Waliser, D., & Maloney, E. (2018). A unified moisture mode framework for seasonality of the Madden–Julian Oscillation. *Journal of Climate*, *31*(4), 215–224. https://doi.org/10.1175/JCLI-D-17-0671.1

Jiang, X., Li, T., & Wang, B. (2004). Structures and mechanisms of the northward propagating boreal summer intraseasonal oscillation. *Journal of Climate*, *17*, 1022–1039. https://doi.org/10.1175/1520-0442(2004)017<1022:SAMOTN>2.0.CO;2

Jiang, X., Waliser, D. E., Xavier, P. K., Petch, J., Klingaman, N. P., Woolnough, S. J., et al. (2015). Vertical structure and physical processes of the Madden-Julian Oscillation: Exploring key model physics in climate simulations. *Journal of Geophysical Research: Atmospheres*, *120*, 4718–4748. https://doi.org/10.1002/2014JD022375

Jones, C., Waliser, D. E., Lau, K. M., & Stern, W. (2004). Global occurrences of extreme precipitation and the Madden-Julian Oscillation: Observations and predictability. *Journal of Climate*, *17*, 4575–4589. https://doi.org/10.1175/3238.1

Kikuchi, K., Kodama, C., Nasuno, T., Nakano, M., Miura, H., Satoh, M., et al. (2017). Tropical intraseasonal oscillation simulated in an AMIP-type experiment by NICAM. *Climate Dynamics*, *48*, 2507–2528. https://doi.org/10.1007/s00382-016-3219-z

Kikuchi, K., & Wang, B. (2010). Formation of tropical cyclones in the Northern Indian Ocean associated with two types of tropical intraseasonal oscillation modes. *Journal of the Meteorological Society of Japan*, *88*, 475–496. https://doi.org/10.2151/jmsj.2010-313

Kikuchi, K., Wang, B., & Kajikawa, Y. (2012). Bimodal representation of the tropical intraseasonal oscillation. *Climate Dynamics*, *38*, 1989–2000. https://doi.org/10.1007/s00382-011-1159-1

Kiladis, G. N., Dias, J., Straub, K. H., Wheeler, M. C., Tulich, S. N., Kikuchi, K., et al. (2014). A comparison of OLR and circulation-based indices for tracking the MJO. *Monthly Weather Review*, *142*, 1697–1715. https://doi.org/10.1175/MWR-D-13-00301.1

Kim, D., Sperber, K., Stern, W., Waliser, D., Kang, I., Maloney, E., et al. (2009). Application of MJO simulation diagnostics to climate models. *Journal of Climate*, *22*, 6413–6436. https://doi.org/10.1175/2009JCLI3063.1

Kim, D., Xavier, P., Maloney, E., Wheeler, M., Waliser, D., Hendon, H., et al. (2014). Process-oriented MJO simulation diagnostic: Moisture sensitivity of simulated convection. *Journal of Climate*, *27*, 5379–5395. https://doi.org/10.1175/jcli-d-13-00497.1

Klotzbach, P. J. (2014). The Madden–Julian Oscillation's impacts on worldwide tropical cyclone activity. *Journal of Climate*, *27*, 2317–2330. https://doi.org/10.1175/JCLI-D-13-00483.1

Kobayashi, S., Ota, Y., Harada, Y., Ebita, A., Moriya, M., Onoda, H., et al. (2015). The JRA-55 reanalysis: General specifications and basic characteristics. *Journal of the Meteorological Society of Japan. Ser. II*, *93*, 5–48. https://doi.org/10.2151/jmsj.2015-001

Kodama, C., Yamada, Y., Noda, A. T., Kikuchi, K., Kajikawa, Y., Nasuno, T., et al. (2015). A 20-year climatology of a NICAM AMIP-type simulation. *Journal of the Meteorological Society of Japan. Ser. II*, *93*, 393–424. https://doi.org/10.2151/jmsj.2015-024

Lau, K. M., & Chan, P. H. (1985). Aspects of the 40–50 day oscillation during the northern winter as inferred from outgoing longwave radiation. *Monthly Weather Review*, *113*, 1889–1909. https://doi.org/10.1175/1520-0493(1985)113<1889:AOTDOD>2.0.CO;2

Lau, K. M., & Chan, P. H. (1986). Aspects of the 40–50 day oscillation during the northern summer as inferred from outgoing longwave radiation. *Monthly Weather Review*, *114*, 1354–1367. https://doi.org/10.1175/1520-0493(1986)114<1354:AOTDOD>2.0.CO;2

Lau, N., Held, I. M., & Neelin, J. D. (1988). The Madden-Julian Oscillation in an idealized general circulation model. *Journal of the Atmospheric Sciences*, *45*, 3810–3832. https://doi.org/10.1175/1520-0469(1988)045<3810:TMJOIA>2.0.CO;2

Liebmann, B., & Smith, C. A. (1996). Description of a complete (interpolated) outgoing longwave radiation dataset. *Bulletin of the American Meteorological Society*, *77*, 1275–1277.

Madden, R. A., & Julian, P. R. (1971). Detection of a 40–50 day oscillation in the zonal wind in the tropical Pacific. *Journal of the Atmospheric Sciences*, *28*, 702–708. https://doi.org/10.1175/1520-0469(1971)028<0702:DOADOI>2.0.CO;2

Madden, R. A., & Julian, P. R. (1972). Description of global-scale circulation cells in the tropics with a 40–50 day period. *Journal of the Atmospheric Sciences*, *29*, 1109–1123. https://doi.org/10.1175/1520-0469(1972)029<1109:DOGSCC>2.0.CO;2

Matsueda, S., & Takaya, Y. (2015). The global influence of the Madden–Julian Oscillation on extreme temperature events. *Journal of Climate*, *28*, 4141–4151. https://doi.org/10.1175/JCLI-D-14-00625.1

Miyakawa, T., Satoh, M., Miura, H., Tomita, H., Yashiro, H., Noda, A. T., et al. (2014). Madden–Julian Oscillation prediction skill of a new-generation global model demonstrated using a supercomputer. *Nature Communications*, *5*(3769). https://doi.org/10.1038/ncomms4769

Nakano, M., Kubota, H., Miyakawa, T., Nasuno, T., & Satoh, M. (2017). Genesis of super cyclone pam (2015): Modulation of low-frequency large-scale circulations and the Madden-Julian Oscillation by sea surface temperature anomalies. *Monthly Weather Review*, *145*, 3143–3159. https://doi.org/10.1175/MWR-D-16-0208.1

Nakano, M., Sawada, M., Nasuno, T., & Satoh, M. (2015). Intraseasonal variability and tropical cyclogenesis in the western North Pacific simulated by a global nonhydrostatic atmospheric model. *Geophysical Research Letters*, *42*, 565–571. https://doi.org/10.1002/2014GL062479

Nakazawa, T. (2006). Madden-Julian Oscillation activity and typhoon landfall on Japan in 2004. *SOLA*, *2*, 136–139. https://doi.org/10.2151/sola.2006-035

Neena, J. M., Waliser, D., & Jiang, X. N. (2017). Model performance metrics and process diagnostics for boreal summer intraseasonal variability. *Climate Dynamics*, *48*, 1661–1683. https://doi.org/10.1007/s00382-016-3166-8

Pai, D. S., Bhate, J., Sreejith, O. P., & Hatwar, H. R. (2011). Impact of MJO on the intraseasonal variation of summer monsoon rainfall over India. *Climate Dynamics*, *36*, 41–55. https://doi.org/10.1007/s00382-009-0634-4

Ren, P., Ren, H. L., Fu, J. X., Wu, J., & Du, L. (2018). Impact of boreal summer intraseasonal oscillation on rainfall extremes in southeastern China and its predictability in CFSv2. *Journal of Geophysical Research: Atmospheres*, *123*, 4423–4442. https://doi.org/10.1029/2017JD028043

Sabeerali, C. T., Ramu Dandi, A., Dhakate, A., Salunke, K., Mahapatra, S., & Rao, S. A. (2013). Simulation of boreal summer intraseasonal oscillations in the latest CMIP5 coupled GCMs. *Journal of Geophysical Research: Atmospheres*, *118*, 4401–4420. https://doi.org/10.1002/jgrd.50403

Satoh, M., Matsuno, T., Tomita, H., Miura, H., Nasuno, T., & Iga, S. (2008). Nonhydrostatic icosahedral atmospheric model (NICAM) for global cloud resolving simulations. *Journal of Computational Physics*, *227*, 3486–3514. https://doi.org/10.1016/j.jcp.2007.02.006

Satoh, M., Tomita, H., Yashiro, H., Miura, H., Kodama, C., Seiki, T., et al. (2014). The non-hydrostatic icosahedral atmospheric model: Description and development. *Progress in Earth and Planetary Science*, *1*(18). https://doi.org/10.1186/s40645-014-0018-1

Sobel, A., & Maloney, E. (2012). an idealized semi-empirical framework for modeling the Madden–Julian Oscillation. *Journal of the Atmospheric Sciences*, *69*, 1691–1705. https://doi.org/10.1175/JAS-D-11-0118.1

Sobel, A., & Maloney, E. (2013). Moisture modes and the eastward propagation of the MJO. *Journal of the Atmospheric Sciences*, *70*, 187–192. https://doi.org/10.1175/JAS-D-12-0189.1

Swinbank, R., Palmer, T. N., & Davey, M. K. (1988). Numerical simulations of the Madden and Julian Oscillation. *Journal of the Atmospheric Sciences*, *45*, 774–788. https://doi.org/10.1175/1520-0469(1988)045<0774:NSOTMA>2.0.CO;2

Szekely, E., Giannakis, D., & Majda, A. J. (2016). Extraction and predictability of coherent intraseasonal signals in infrared brightness temperature data. *Climate Dynamics*, *46*, 1,473–1,502. https://doi.org/10.1007/s00382-015-2658-2

Taylor, K. E. (2001). Summarizing multiple aspects of model performance in a single diagram. *Journal of Geophysical Research*, *106*, 7183–7192. https://doi.org/10.1029/2000JD900719

Taylor, K. E., Stouffer, R. J., & Meehl, G. A. (2012). An overview of CMIP5 and the experiment design. *Bulletin of the American Meteorological Society*, *93*, 485–498. https://doi.org/10.1175/BAMS-D-11-00094.1

Thompson, D. B., & Roundy, P. E. (2013). The relationship between the Madden–Julian Oscillation and U.S. violent tornado outbreaks in the spring. *Monthly Weather Review*, *141*, 2087–2095. https://doi.org/10.1175/MWR-D-12-00173.1

Tomita, H., & Satoh, M. (2004). A new dynamical framework of nonhydrostatic global model using the icosahedral grid. *Fluid Dynamics Research*, *34*, 357–400. https://doi.org/10.1016/j.fluiddyn.2004.03.003

Wang, B., Lee, S. S., Waliser, D. E., Zhang, C. D., Sobel, A., Maloney, E., et al. (2018). Dynamics-oriented diagnostics for the Madden-Julian Oscillation. *Journal of Climate*, *31*(3), 3117–3135. https://doi.org/10.1175/jcli-d-17-0332.1

Wang, B., & Rui, H. (1990). Synoptic climatology of transient tropical intraseasonal convection anomalies: 1975–1985. *Meteorology and Atmospheric Physics*, *44*, 43–61. https://doi.org/10.1007/BF01026810

Wang, B., & Xie, X. (1997). A model for the boreal summer intraseasonal oscillation. *Journal of the Atmospheric Sciences*, *54*, 72–86. https://doi.org/10.1175/1520-0469(1997)054<0072:AMFTBS>2.0.CO;2

Weare, B. C., & Nasstrom, J. S. (1982). Examples of extended empirical orthogonal function analyses. *Monthly Weather Review*, *110*, 481–485. https://doi.org/10.1175/1520-0493(1982)110<0481:EOEEOF>2.0.CO;2

Wu, R. G., & Wang, B. (2000). Interannual variability of summer monsoon onset over the western North Pacific and the underlying processes. *Journal of Climate*, *13*, 2483–2501. https://doi.org/10.1175/1520-0442(2000)013<2483:IVOSMO>2.0.CO;2

Xavier, P., Rahmat, R., Cheong, W. K., & Wallace, E. (2014). Influence of Madden-Julian Oscillation on Southeast Asia rainfall extremes: Observations and predictability. *Geophysical Research Letters*, *41*, 4406–4412. https://doi.org/10.1002/2014GL060241

Yoshida, R., Kajikawa, Y., & Ishikawa, H. (2014). Impact of boreal summer intraseasonal oscillation on environment of tropical cyclone genesis over the western North Pacific. *SOLA*, *10*, 15–18. https://doi.org/10.2151/sola.2014-004

Zhang, C., & Dong, M. (2004). Seasonality in the Madden–Julian Oscillation. *Journal of Climate*, *17*, 3169–3180. https://doi.org/10.1175/1520-0442(2004)017<3169:SITMO>2.0.CO;2